

Geomagnetic Deep Sounding in and around the Kenya Rift Valley

R. J. Banks and P. Ottey

(Received 1973 July 9)

Summary

Six magnetic variometers were installed at sites along a 300 km east–west line, crossing the eastern branch of the East African Rift Valley near the Equator. The instruments were operated from March to May 1971, during which time four magnetic disturbances were recorded.

Transfer functions have been computed for each station, and are presented both as real and imaginary induction arrows and in an alternative ‘maximum and minimum’ form. They show that a relatively shallow concentration of induced current flows along the axis of the rift valley. However, the anomaly is not symmetric, and the phase of the response shows a complex behaviour on the east side of the Rift.

The computer program of Jones and Pascoe has been used to compute the response of two-dimensional conductivity models. The type of model that fits the experimental data involves a strip of high conductivity material at a depth of no more than 20 km beneath the floor of the rift with, in addition, a thick slab (100 km) of material of more moderate conductivity at a depth of 50 km beneath the eastern flanks of the rift. The lateral extent of this slab was not precisely defined by the 1971 experiment, but it may well be several hundred kilometres.

The two regions of high conductivity are interpreted as zones of partial melting in the upper mantle. Their positions coincide with the regions of most recent (late Quaternary) volcanism.

1. Introduction

Seismic and gravity investigations show clear evidence of an anomalous structure in the crust and upper mantle beneath the Kenya dome and the eastern branch of the rift valley that runs across it. Knopoff & Schlue (1972) and Long *et al.* (1972) have used the dispersion of Rayleigh waves along paths between Nairobi and Addis Ababa to determine the shear velocity distribution. The great circle path between these two seismic observatories passes some distance to the east of the graben, but still beneath the dome. The crustal structure appears to be similar to that of the African shield model of Gumper & Pomeroy (1970), but the mantle has an abnormally low shear velocity of 4.25 km s^{-1} at depths of 50–200 km (as compared with values of 4.6–4.8 km s^{-1} for Gumper & Pomeroy’s model). It is possible that there is a cap of normal mantle material beneath the crust, but the data are not good enough to resolve this model from one in which the low velocity zone extends right up to the Mohorovicic discontinuity.

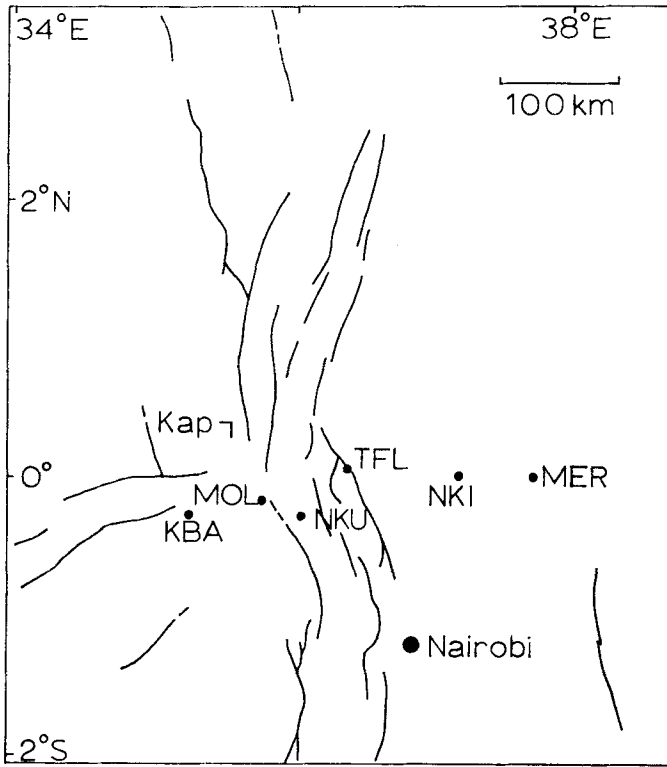


FIG. 1. Location of the magnetometer sites relative to major rift faults. *KBA*: Kabianga; *MOL*: Molo; *NKU*: Nakuru; *TFL*: Thomson's Falls; *NKI*: Nanyuki; *MER*: Meru; *Kap*: Kaptagat.

There is strong evidence to suggest that the anomalous mantle material does not extend very far to the west of the Gregory rift. Long *et al.* (1972) have presented some preliminary analysis of data from their seismic array station at Kaptagat, on the western escarpment of the rift valley (see Fig. 1). Measurements of the apparent velocity of P waves from regional earthquakes occurring to the west of the Gregory rift indicate a normal crust (thickness about 35 km and P velocities in the range $5.8\text{--}6.3\text{ km s}^{-1}$) immediately to the west of the array station, underlain by mantle with a P_n velocity of 7.9 km s^{-1} . However, the apparent velocities of teleseismic P arrivals show a very considerable variation with the source azimuth, which can be explained by postulating the existence of a prism of low velocity material, thinning to the west beneath the western wall of the rift. Other evidence (the results of the seismic refraction experiment and the gravity surveys of the axial zone of the rift, discussed later) rules out the possibility of this prism being in the crust; if it is in the mantle it is most likely to be the westward continuation of the low shear velocity zone detected by the surface wave measurements. Long *et al.* suggest that the prism may have a P velocity of 7 km s^{-1} or less. The dips of both the upper and lower boundaries of the prism seem to be quite considerable; Backhouse (1972) estimates that the upper face dips at about 40° away from the rift, while the lower face dips by a similar amount towards the rift.

Further evidence of the existence of a zone of low velocity material in the mantle comes from the measurement of the delays and relative delays of teleseismic P waves (Fairhead & Girdler 1971; Long *et al.* 1972). The delays observed at Nairobi and Addis Ababa are large (2–3 s) and positive, but at Lwiro on the western rift, in the

Congo, the delay is only +1 s, suggesting that the anomalous zone is less extensive there. The delay at Kaptagat, relative to Bulawayo, is about +2 s (Backhouse 1972), and can be interpreted as being due to a thickness of about 100 km of material with P velocity 7 km s^{-1} . Fairhead & Girdler (1971) found that P waves travelling through the top of the mantle on paths along or near the rift north of 5° S suffer large positive delays. Along paths to the south, or even running across the region between the two branches of the rift, the delays are usually small or negative. Other evidence that the low velocity mantle is restricted to the northern part of the eastern rift, and to the extreme northern part of the western rift, has come from studies of the propagation of the phase S_n . Gumper & Pomeroy (1970) found that S_n propagates across the rift south of 10° S , but not across the northern part, north of the equator. Between 10° S and 0° , S_n propagates along some paths, mainly those across the rift, but not along others. Gumper & Pomeroy follow Molnar & Oliver (1969) in interpreting regions across which S_n does not propagate as having a mantle with an unusually low Q . The general correspondence in East Africa between regions of poor S_n propagation and regions underlain by low velocity mantle strongly suggests that it is the low velocity material which has the low Q . The preferred explanation of the broad negative Bouguer gravity anomaly associated with the rift system is a zone of low density material in the upper mantle beneath the rift (Khan & Mansfield 1971; Searle 1970). It is to be expected that material with low P and S velocities and a low Q will also have a low density relative to normal mantle, and it might be thought that the gravity data offered the best means of mapping the lateral extent of the anomalous mantle. Unfortunately it seems difficult in practice to estimate the contribution to the negative gravity anomaly from the low density volcanic rocks.

Superimposed on the broad negative gravity anomaly is a smaller positive anomaly between 40 and 80 km wide, apparently confined to the graben, and extending more or less continuously from 1.25° S to 0.25° N . The positive anomaly has been interpreted as being caused by an intrusion, or series of intrusions, of mantle-derived material between 10 and 20 km wide, and reaching to within 2–3 km of the rift floor (Searle 1970; Baker & Wohlenberg 1971). The intrusive body is considered to be an upward extension of the anomalous zone in the mantle. An alternative explanation of the anomaly is that it is caused by the infilling of the rift by dense lavas. Searle (1970) estimates that 3–6 km of infill with density 3000 kg m^{-3} would be required, and rejects such a thickness as being unreasonable in the light of geological estimates. A seismic refraction experiment between Lake Rudolf and Lake Hannington (Griffiths *et al.* 1971; Griffiths 1972) detected high velocity material (P velocity 6.4 km s^{-1}) at 3 km depth, underlain by material of velocity 7.5 km s^{-1} at a depth of about 20 km. Long *et al.* (1972) find apparent velocities of 7.1 km s^{-1} for P waves recorded at Kaptagat from earthquakes in and to the east of the rift, and suggest that the 7.5 km s^{-1} refractor may be a high velocity upper surface of the anomalous zone in the mantle that has already been discussed.

The overall structure of the crust and upper mantle beneath the rift that emerges from the geophysical investigations is summarized in Fig. 2. This diagram represents a model that is, if nothing more, broadly compatible with the bulk of the data. It should give a reasonable picture of the structure on a profile across the rift at about 0° .

The most plausible explanation of the low velocity, low density zone is that it consists of partially melted mantle material. Whether the anomalous zone is caused by partial melting or by the more direct effects of high temperatures, its electrical conductivity should be higher than that of the normal mantle. The experiments of Presnall, Simmons & Porath (1972) show that the conductivity of basalt increases by 2–3 orders of magnitude on melting, and it is likely that a similar result will hold for peridotite. In fact, if peridotite is partially melted, the interstitial liquid on moderate amounts of melting will have the composition of basalt, and the compositional difference will also tend to raise the bulk conductivity. In any case, it should be possible to map

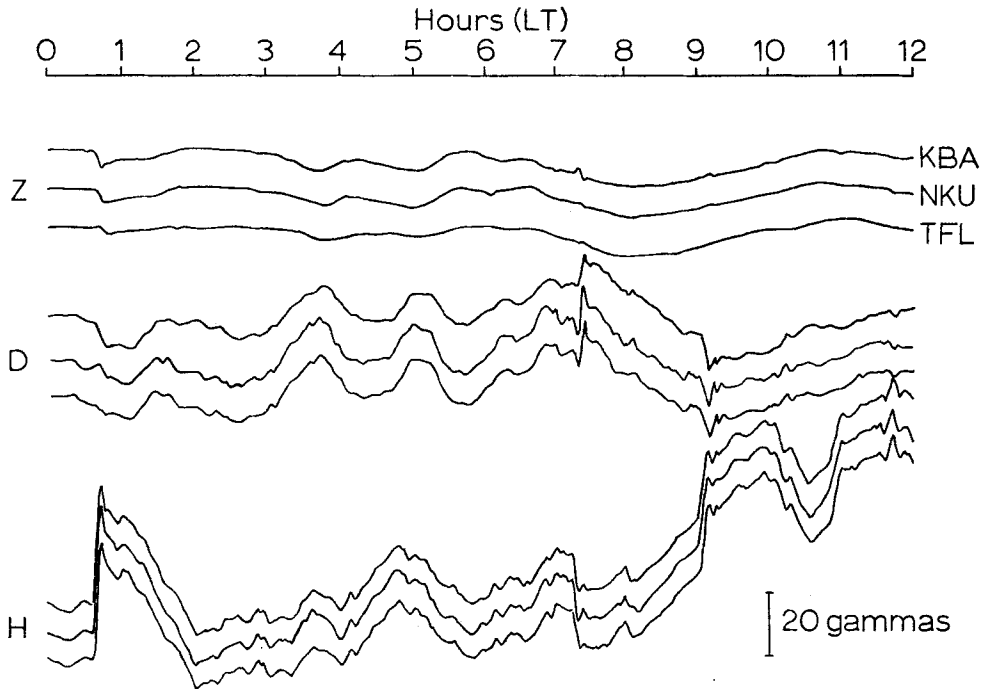


FIG. 3. Simultaneous magnetograms for the magnetic storm of 1971 April 4.

and smallest to the east of the rift (Thomson's Falls). At shorter periods, the variations appear to reverse direction between Kabianga and Thomson's Falls (e.g. the oscillatory variation at 0720 hr).

4. Calculation of transfer functions

Because of the lack of simultaneous data, we decided to calculate single station transfer functions for as many disturbances as had been recorded at each station. The transfer functions $A(f)$ and $B(f)$, defined by the equation

$$Z_c(f) = A(f)H(f) + B(f)D(f) \tag{1}$$

were computed from spectra and cross-spectra of $Z(t)$, $H(t)$ and $D(t)$ according to the formulae given by Banks (1973). The implications of using equation (1) and the assumptions which must be satisfied for the transfer estimates to be meaningful are also discussed in the latter paper. Among the assumptions made is that any normal vertical field does not correlate with the horizontal field components; otherwise it is difficult to make satisfactory estimates of $A(f)$ and $B(f)$.

Three 12-hr records of magnetic storms, digitized at an interval of 1 min, were available for Kabianga, and two such records at each of the other stations. The spectra were pre-whitened by a high-pass filter to guard against the effects of leakage from the large amount of power at the first few frequency estimates. The resolution of the spectra was $10^{-2} \text{ c min}^{-1}$. Transfer estimates were calculated for individual records and then averaged.

4.1 Real and imaginary induction vectors

The quantities $A(f)$ and $B(f)$ are in general complex. One way of presenting them is to separate real and imaginary parts, and to calculate the lengths and directions

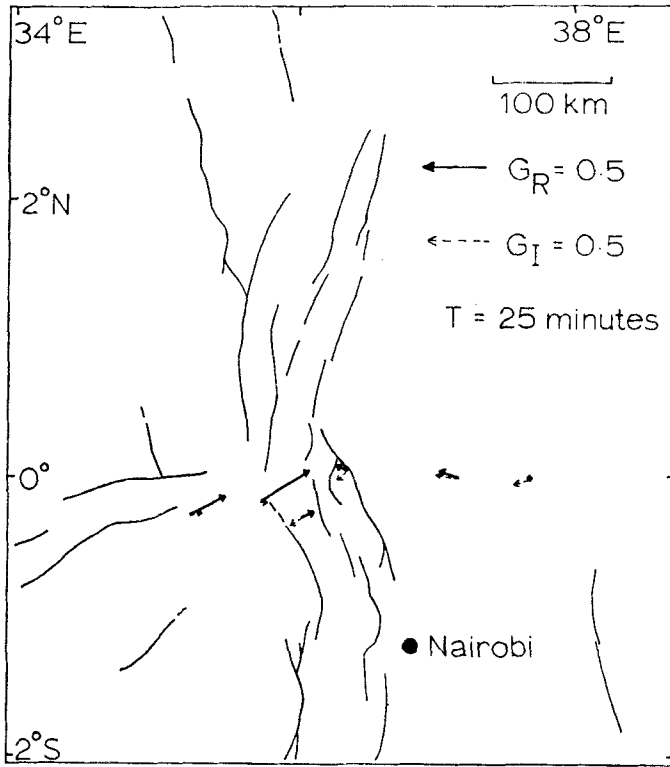


FIG. 4. Real and imaginary induction vectors for a period of 25 min.

of induction arrows or vectors. The vectors calculated in this way define the direction of the horizontal field disturbance with which the vertical field disturbance shows maximum correlation, and should point away from anomalous internal concentrations of current. Their interpretation is discussed by, among others, Hyndman & Cochrane (1972) and Banks (1973). The usual convention is for the arrows to point towards the internal currents; consequently, in Fig. 4, which shows real and imaginary induction vectors at a period of 25 min, the azimuths of both real and imaginary vectors have been changed by 180° . The lengths of the arrows are proportional to the amplitude of the correlated vertical field associated with a unit amplitude disturbance in the horizontal field.

The real induction vectors quite clearly indicate a concentration of current flowing from NNW to SSE along the rift valley. The direction of the real vectors reverses between Nakuru and Thomson's Falls, and the correlated vertical field amplitude reaches a maximum at Molo to the west of the rift and at Nanyuki to the east. However, the anomaly is not symmetric. The maximum vertical field amplitudes on the west side of the rift are two to three times the maximum amplitudes on the east side suggesting that the conducting body must extend eastwards away from the rift axis. It is unlikely that the asymmetry could be due to contamination of the transfer estimates by a normal vertical field. Any systematic spatial variation in the normal vertical field would be in a predominantly north-south direction at these low latitudes; substantial changes in an east-west direction in a distance of 300 km are unlikely.

The imaginary vectors have generally the same azimuth as the real vectors, and are probably associated with the same conductivity anomaly. On the west side of the rift, their magnitude is small compared with that of the real vectors, indicating that the

vertical field variations are almost in phase with the horizontal. On the east side, however, the length of the imaginary vector is comparable with that of the real vector, and at Meru the correlated field is almost entirely imaginary, corresponding to a 90° phase difference between the vertical and horizontal components.

In such circumstances, where the phase of the anomalous fields differs substantially from zero, the division of the response into real and imaginary parts seems rather artificial, and is not the most informative or telling way of presenting the data.

4.2 Maximum and minimum responses

One way of presenting the information contained in equation (1) would be to compute the quantity $Z_c(f)Z_c^*(f)$ for a horizontal variation of unit amplitude and zero phase at azimuth θ . The correlated vertical field associated with such a horizontal disturbance would be, according to equation (1)

$$Z_c(f) = A(f) \cos \theta + B(f) \sin \theta \tag{2}$$

so that the square of the modulus of Z_c would be

$$Z_c(f)Z_c^*(f) = (A(f) \cos \theta + B(f) \sin \theta)(A^*(f) \cos \theta + B^*(f) \sin \theta). \tag{3}$$

The dependence of $Z_c(f)Z_c^*(f)$ on θ can be represented by a polar response diagram. The value of θ for which $Z_c(f)Z_c^*(f)$ is a maximum can be found by differentiating equation (3) with respect to θ , and setting the result equal to zero. We find

$$\tan 2\theta_p = \frac{A(f)B^*(f) + A^*(f)B(f)}{A(f)A^*(f) - B(f)B^*(f)} \tag{4}$$

defines the direction in which the modulus of the response is a maximum (or minimum).

The response will be a minimum (or maximum) along an axis at 90° to that defined by equation (4), and the phase of the response along the two axes will differ by 90°. The analysis is in many ways similar to that used in the synthesis of elliptical polarisation from two simple harmonic motions along orthogonal axes, as Everett & Hyndman (1967) pointed out when they first suggested this technique. However, in this case, the ellipse itself has no particular significance, since the simple harmonic oscillations combined in the right-hand side of equation (1) are not orthogonal to one another, but are both in the vertical direction. For this reason, any reference to an ‘induction ellipse’ is misleading.

A more straightforward way of looking at the problem is to consider it as one of referring equation (1) to a new set of axes H' and D' , such that the modulus of the response is a maximum along the H' axis and a minimum along the D' axis. We can then rewrite equation (1) in terms of these new co-ordinates

$$Z_c(f) = G_p(f)H'(f) + G_l(f)D'(f). \tag{5}$$

It seems to us that the representation of the response in terms of the pair of complex quantities $G_p(f)$ and $G_l(f)$ is a particularly useful one, since it can be related directly to an interpretation in terms of the perturbation of the induced current flow by a two-dimensional conductivity structure. In such an electromagnetic induction problem, vertical field variations are associated with the E polarization mode (Jones & Price 1970), and correlate only with horizontal field variations in a direction perpendicular to the strike of the conductor. Vertical field variations should not correlate at all with horizontal magnetic field variations in a direction parallel to the strike of the conductor. Consequently, in a true two-dimensional situation, we should find that H' , as calculated above, defines an axis perpendicular to the strike of the conductor, and $G_l(f) = 0$. By computing the response $G_p(f)$, we are incorporating as much of the observed responses $A(f)$ and $B(f)$ as is compatible with the two-dimensional assump-

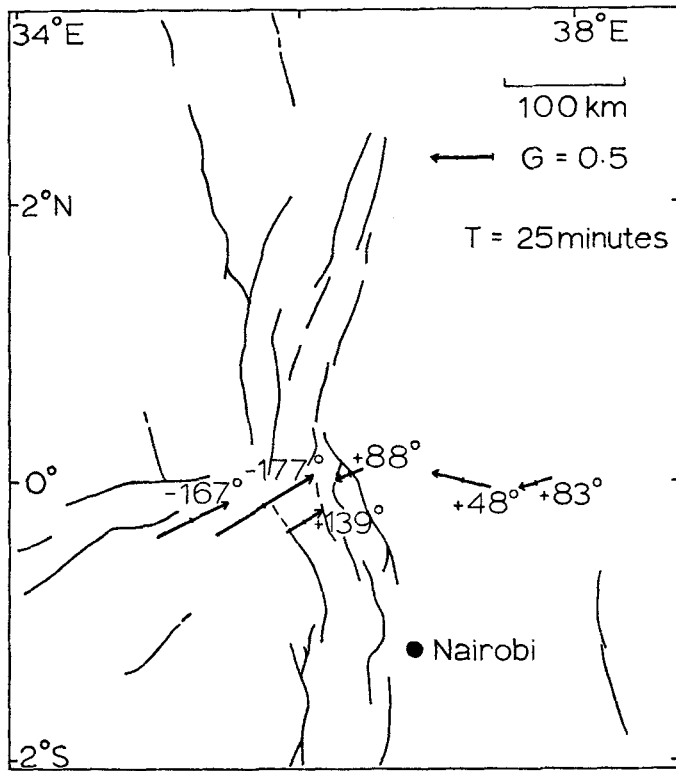


FIG. 5. Representation of maximum and minimum responses at a period of 25 min.

tion. The relative magnitudes of $G_p(f)$ and $G_l(f)$ should be a measure of how far the two-dimensional assumption is justified.

We have calculated maximum and minimum response parameters for the six stations, using the same data as for the induction vectors. The results obtained at a period of 25 min are displayed in Fig. 5.

The presentation is similar to that of the induction vectors. The lines centred on each station are drawn in the directions of the H' and D' axes, and their lengths are proportional to $|G_p|$ and $|G_l|$. However, both the positive and negative axes are shown, with the result that the length of the line is twice that of the induction vector. The phase of G_p along the east pointing axis is shown by its side, and a further indication of the phase is provided by the arrow, marked on the H' axis for which the phase of G_p lies between 90° and 180° or between -90° and -180° . Defined in this way, the arrow points in the same direction as the induction vector, i.e. towards concentrations of current.

A comparison of Figs 4 and 5 shows that the new method of presentation does resolve the confusion that might result from a separate consideration of the real and imaginary induction vectors. Both the real and imaginary responses appear to be associated with the same anomalous distribution of conductivity, but the Z/H phase of the anomaly changes from -170° on the west of the rift to $+48^\circ$ at Nanyuki, and $+83^\circ$ at Meru. In all cases, $|G_l|$ is small compared with $|G_p|$, and an interpretation in terms of a two-dimensional conductivity structure would appear to be justified.

Figs 6-9 show the frequency dependence of the response at two representative stations, Kabianga to the west of the rift, and Nanyuki to the east. The modulus of the response (Figs 6 and 8) does not show any substantial variation with frequency

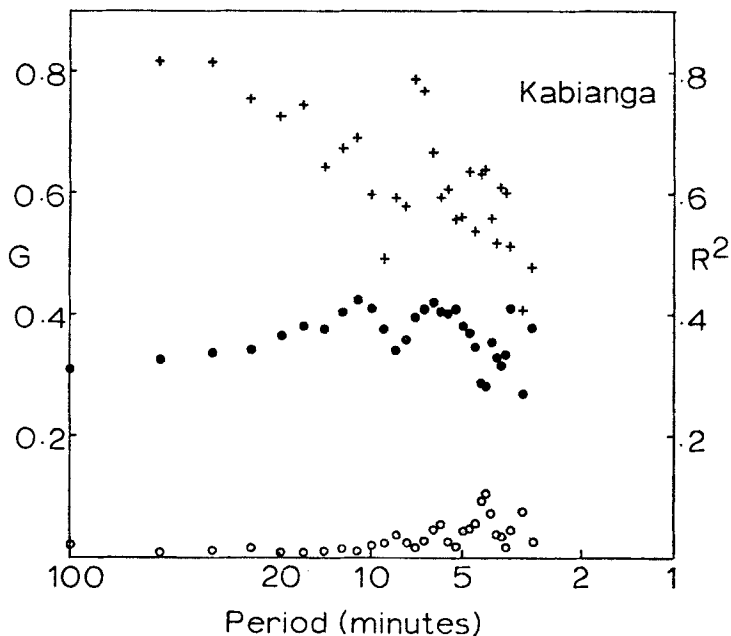


FIG. 6. Maximum (closed circles) and minimum (open circles) responses at Kabianga as a function of period. The crosses represent the coherence $R^2(f)$ between $Z(f)$ and $Z_e(f)$.

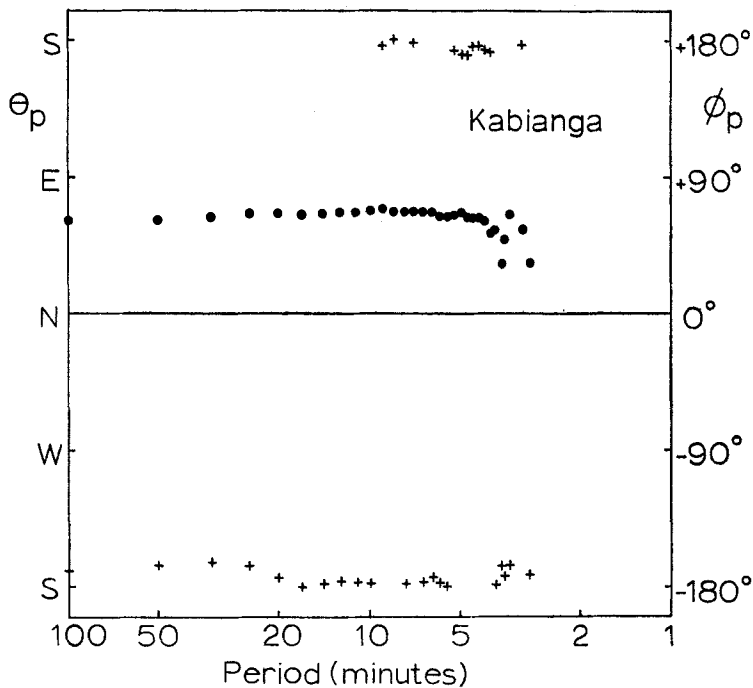


FIG. 7. Azimuth (circles) and phase (crosses) of the maximum response axis at Kabianga as a function of period.

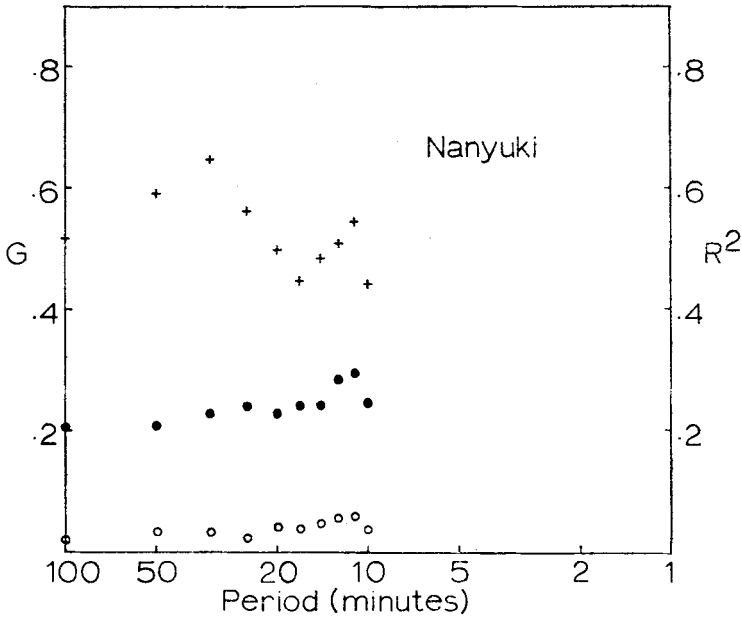


FIG. 8. Maximum and minimum responses at Nanyuki as a function of period. (Symbols as for Fig. 6).

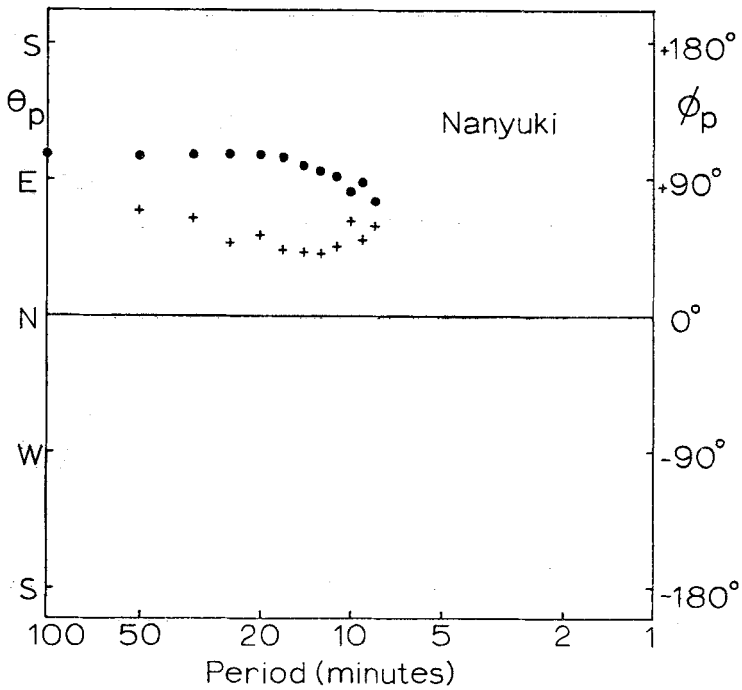


FIG. 9. Azimuth and phase of the maximum response axis at Nanyuki. (Symbols as for Fig. 7)

over the limited range for which estimates are available. There is a slight tendency at both stations for $|G_p|$ to peak at a period of about 10 min. As a measure of the goodness of fit of $Z(f)$ to the equation $Z_c(f) = A(f)H(f) + B(f)D(f)$, we have computed the coherence $R^2(f)$ between $Z(f)$ and $Z_c(f)$, and have rejected all response estimates for which $R^2(f)$ is less than 0.4.

The azimuths (θ_p) of the H' axis are very consistent in direction (Figs 7 and 9). The phase of $G_p(\phi_p)$ reaches a minimum of 40° at Nanyuki at periods between 10 and 20 min. It appears that the maximum response of at least one part of the anomaly is in this period range.

5. Model calculations

We have used the computer program of Jones & Pascoe (1971) to calculate the response at the Earth's surface of two-dimensional conductivity structures. The program has been slightly modified so as to compute the amplitude ratio and phase difference between the vertical component and the transverse horizontal component of the field at each station. This enables a direct comparison to be made between the results of the model calculations and our response estimates $G_p(f)$. The comparison was made at a period of 25 min only. The response appears to vary fairly slowly with frequency, and the values at 25 min seem representative of the frequency range $0.01\text{--}0.1\text{ c min}^{-1}$. The conductivity structures have been kept as simple as possible, with models being built up from simple rectangular prisms. The restriction to simple shapes makes it easier to determine the way in which the surface response is affected by changes in the model parameters.

Certain essential features of the conductivity structure are apparent from the response data presented in Section 4:

(1) The western edge of the conducting body lies beneath the western scarp of the rift.

(2) The asymmetry of the anomaly indicates that the conductor must extend eastwards beyond the eastern escarpment of the rift.

(3) The concentration of current flowing beneath the floor of the rift (indicated by the reversal in direction of the induction arrows, etc.) points to the existence of a good conductor directly beneath the rift floor. The relatively small lateral scale of the anomaly indicates that the source must be fairly shallow, at a depth of not more than a few tens of kilometres.

With a model consisting of an asymmetric prism of conducting material beneath the rift, and directly to the east of it, we were able to explain the shape of the anomaly in $|G_p|$ and also the -170° phase to the west of the rift. However, models which essentially involve a single conducting body beneath the rift give phases close to zero on the east side of the rift. It is pertinent to point out here that, because the amplitude of the vertical field variations is considerably smaller to the east of the rift, the phase estimates there are less reliable than those for stations to the west of the rift. If we reject the phase estimates for stations on the eastern side as unreliable, the anomaly can be explained in terms of a single asymmetric body beneath the rift floor. However, we think that the consistency of the phase estimates at Nanyuki, for example (Fig. 9), is such that the substantial positive phases cannot be dismissed in this way.

In order to explain the data as a whole, a more complex conductivity structure is required, with the eastward extension of the conducting body stretching much further east, and forming a second major conductor in its own right. The interaction of the magnetic fields due to the induced currents flowing in these two bodies can produce the observed complexity in the phase. Fig. 10 shows such a structure, and a comparison between the model response and the observational data. The depth of the conductor beneath the rift (20 km) was chosen to correspond to the depth of the

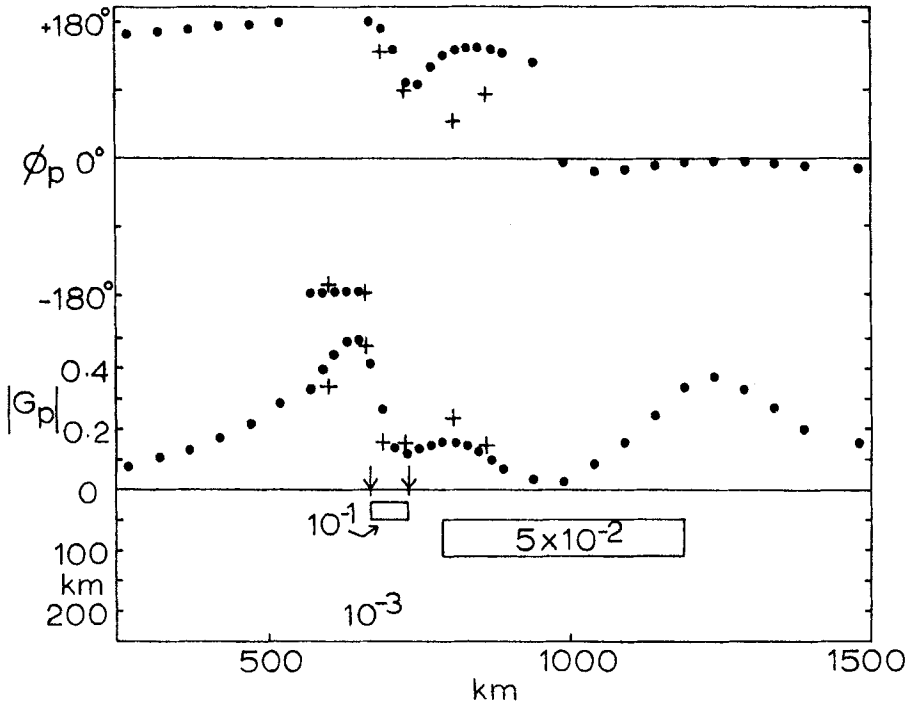


FIG. 10. Deep sub-rift conductor: comparison of the computed response (circles) with the observed response (crosses) at 25-min period. Figures give the conductivity in $\text{ohm}^{-1} \text{m}^{-1}$. Arrows indicate the lateral extent of the rift valley.

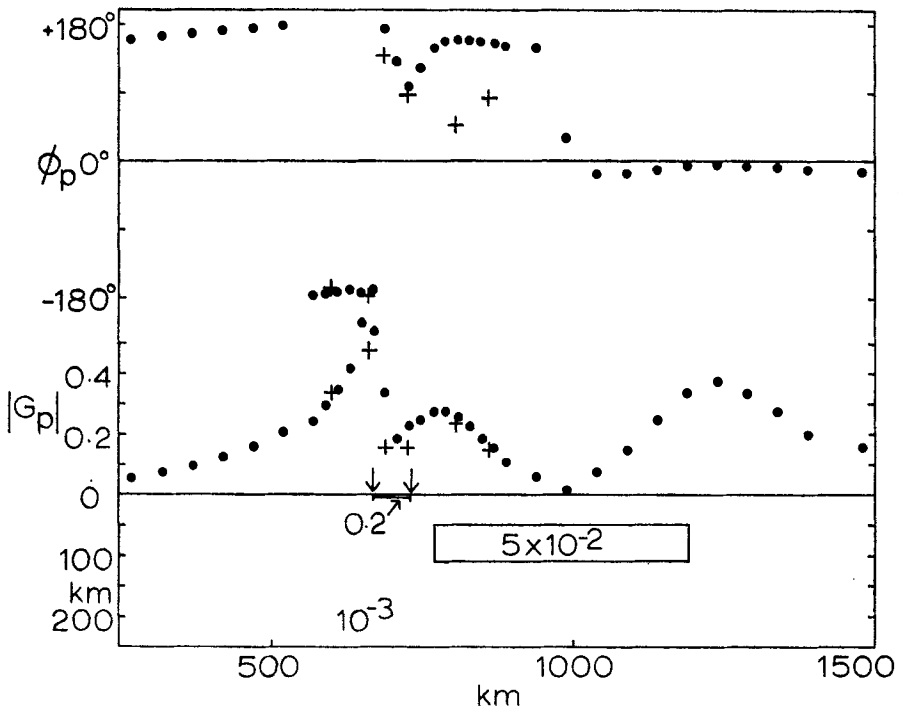


FIG. 11. Shallow sub-rift conductor: comparison of the computed and observed responses at 25-min period.

7.5 km s^{-1} refractor; the eastern conductor was placed at a depth of 50 km to correspond to the low shear velocity zone found in the surface wave analysis.

It should be stressed that there is likely to be a high degree of non-uniqueness in the process of selecting models, especially when, as in this case, we only consider the response at a single frequency. To illustrate this non-uniqueness, we have computed the response of a model in which the sub-rift conductor lies immediately beneath the surface, and has a thickness of only 5 km. A conductivity of $0.2 \text{ ohm}^{-1} \text{ m}^{-1}$ for this body gives just as good a fit (see Fig. 11) to the 25-min period data as the model shown in Fig. 10. However, such a model does not give the right response at a period of 100 min.

In the face of this kind of ambiguity, we did not think it worthwhile to adjust the shape of the conducting bodies either to obtain an exact fit to the observations, or to make them more geologically reasonable.

6. Interpretation

Two distinct models have been found (Figs 10 and 11) with responses that agree with the observational data at a period of 25 min. There are doubtless many other substantially different models that satisfy this criterion. Some of these could be eliminated by checking how they responded at other frequencies. The data obtained in 1971 unfortunately have a limited frequency range, and we have been forced to concentrate on a single representative frequency. However, the lateral position of the two conducting bodies responsible for the anomaly is probably fairly well defined, except for the eastward extent of the eastern conductor. On the other hand, the depth, thickness, and conductivity of the bodies are subject to considerable uncertainty. In order to remove some of this uncertainty, we have to consider what is reasonable in the light of the other geophysical and geological data.

The model shown in Fig. 11, with the rift conductor at the surface, is essentially an attempt to explain the anomaly by an infill of conductive material in the rift graben. The infilling material consists of intercalated lavas, tuffs and thin layers of lake sediments. Drilling for water has shown that the aquifers are in general thin and localized, associated mainly with faulting and fissuring, or with weathered horizons (McCall 1967). It therefore seems highly unlikely that the infilling material could have a bulk conductivity as high as $0.2 \text{ ohm}^{-1} \text{ m}^{-1}$, even if its thickness is as great as 5 km, and the source of the anomaly must be sought at greater depths.

In Section 1, we mentioned the possibility that the low velocity, low density zone indicated by the gravity and seismic experiments was a region of partial melting in the upper mantle. The most telling evidence in favour of such an interpretation is the recent volcanic activity in and around the rift valley, and the associated geothermal activity. Otherwise, an interpretation in terms of lateral variations in the composition of the mantle would be difficult to rule out completely. The other possibility is that the anomalous zone is at an elevated temperature without actual melting having occurred. If we accept that its conductivity is about $0.1 \text{ ohm}^{-1} \text{ m}^{-1}$, a rough lower limit can be set on the temperature by using the results of laboratory experiments on the effect of increasing temperatures on the conductivity of olivines. Duba & Lilley (1972, Fig. 2) have assembled a representative set of laboratory data for olivines with 10 per cent fayalite. Although the conductivity can vary by up to three orders of magnitude at any one temperature, it would seem that a conductivity of $0.1 \text{ ohm}^{-1} \text{ m}^{-1}$ can only be reached at temperatures in excess of 1200°C . At depths of 20–100 km, such temperatures are probably sufficient to cause melting, particularly under wet conditions (Wyllie 1971).

Presnall *et al.* (1972) have carried out experiments which show that the conductivity of basalt increases by two orders of magnitude when it melts. When peridotite is partially melted, the situation is more complicated. For small amounts

of melting, the residual solid material will have roughly the composition of the original peridotite, while the interstitial basaltic fluid will have a relatively high conductivity both because of its composition and because it is molten. The bulk conductivity of the partially melted rock depends critically on the degree of melting. Tolland & Strens (1972) have found that the electrical conductivity of mixtures of conducting and non-conducting materials increases suddenly when the proportion of the conducting phase exceeds a certain critical value, corresponding to the formation of effectively infinite chains of the conducting component. They suggest that in the situation when the conducting phase is an interstitial fluid, the critical composition may be as low as 5 per cent. When the degree of melting exceeds this figure, the conductivity of the bulk material will increase from a value of the same order as that of the non-conducting component to a value of the same order as that of the conducting component. The conductivity of molten basalt at a temperature of 1200 °C is in excess of $1 \text{ ohm}^{-1} \text{ m}^{-1}$ (Presnall *et al.* 1972), so a conductivity of $0.1 \text{ ohm}^{-1} \text{ m}^{-1}$ for partly melted peridotite seems not at all unreasonable.

The lateral and vertical extent of the high conductivity zone beneath the rift valley appears to be much less than that of the low velocity, low density zone detected by the seismic and gravity investigations. A possible explanation is that the conductor represents the part of the mantle where the greatest amount of melting has occurred. Only in a limited region beneath the rift and to the east of it is the concentration of melt sufficiently high to exceed the critical value and cause a high conductivity. In the other regions detected by the seismic and gravity experiments, the mantle may also be partly molten, but the concentration of melt is less than the critical value.

The location of the postulated partial melt zones should show a relation to the most recent volcanic activity, and this is indeed the case. Baker *et al.* (1971) have established a chronology for the volcanic rocks of the Kenyan Rift and they conclude that the most recent volcanic activity is concentrated in two regions:

(1) along the floor of the rift, a late Quaternary phase of mainly trachytic caldera eruptions.

(2) in three areas 150–250 km east of the rift, a late Quaternary phase of multi-centre basalt volcanism.

One of the three multi-centre basalt fields, the Nyambeni range, lies along the line of our profile, above the eastern zone of high conductivity.

7. Conclusions

A preliminary magnetic deep sounding experiment in Kenya appears to have detected two regions of high conductivity (about $0.1 \text{ ohm}^{-1} \text{ m}^{-1}$), one beneath the rift floor at a depth of about 20 km, the other 100 km east of the rift at a depth of about 50 km. These regions of high conductivity are interpreted as being parts of the mantle where the concentration of melt exceeds a critical value. An interpretation in terms of partial melting is supported by the correspondence of the two anomalous zones to the two regions of late Quaternary volcanic activity.

In 1972, a large scale experiment with over 20 magnetometers was carried out. It is hoped that the results of the second experiment will help to show whether the interpretation given here is correct, besides delineating the boundaries of the two anomalous zones in two dimensions rather than one. We also hope that a more detailed study will define more precisely the depths to and thicknesses of the anomalous regions. If they do indeed consist of partially melted mantle material, and form the source from which the most recent volcanic rocks have been derived, it is of particular importance to confirm or disprove the suggested difference in depths of the two partial melt zones. If this difference can be shown to be real, it might help to explain the difference in chemistry of the volcanic rocks, and also the difference in character of the volcanic activity.

If the temperature is in excess of 1000°C at a depth of 20 km, the geothermal gradient should be 50°C km⁻¹, and the heat flow over the rift at least twice the normal value. No heat flow data are as yet available for the eastern rift, but it is clearly important that every effort be made to obtain such confirmation of the thermal state of the mantle.

Acknowledgments

We would like to thank the Government of Kenya for allowing us to carry out this research, and the members of staff at the schools at Meru, Nanyuki, Thomson's Falls, Nakuru, Molo, and Kabianga who helped us by providing sites, and who were very generous with their hospitality. Professor N. Skinner provided us with facilities at the Physics Department at the University of Nairobi, and Dr A. Brock and other members of the staff gave us a great deal of help with local problems. We are very grateful to them. The research was financed by a grant from the Natural Environment Research Council, who also provided a studentship for P.O.

*Department of Environmental Sciences,
University of Lancaster*

References

- Backhouse, R. W., 1972. Ph.D. thesis, University of Durham.
- Baker, B. H., Williams, L. A. J., Miller, J. A. & Fitch, F. J., 1971. *Tectonophysics*, **11**, 191.
- Baker, B. H. & Wohlenberg, J., 1971. *Nature*, **229**, 538.
- Banks, R. J., 1973. *Phys. Earth Planet. Int.*, **7**, 339.
- Duba, A. & Lilley, F. E. M., 1972. *J. geophys. Res.*, **77**, 7100.
- Everett, J. E. & Hyndman, R. D., 1967. *Phys. Earth Planet Int.*, **1**, 24.
- Fairhead, J. D. & Girdler, R. W., 1971. *Geophys. J. R. astr. Soc.*, **24**, 271.
- Gough, D. I. & Reitzel, J. S., 1967. *J. Geomagn. Geoelect., Kyoto*, **19**, 203.
- Griffiths, D. H., King, R. F., Khan, M. A. & Blundell, D. J., 1971. *Nature Phys. Sci.*, **229**, 69.
- Griffiths, D. H., 1972. *Tectonophysics*, **15**, 151.
- Gumper, F. & Pomeroy, P. W., 1970. *Bull. seism. Soc. Am.*, **60**, 651.
- Jones, F. W. & Pascoe, L. J., 1971. *Geophys. J. R. astr. Soc.*, **24**, 3.
- Hyndman, R. D. & Cochrane, N. A., 1972. *Geophys. J. R. astr. Soc.*, **25**, 425.
- Jones, F. W. & Price, A. T., 1970. *Geophys. J. R. astr. Soc.*, **20**, 317.
- Khan, M. A. & Mansfield, J., 1971. *Nature Phys. Sci.*, **229**, 72.
- Knopoff, L. & Schlue, J. W., 1972. *Tectonophysics*, **15**, 157.
- Long, R. E., Backhouse, R. W., Maguire, P. K. H. & Sundarlingham, K., 1972. *Tectonophysics*, **15**, 165.
- McCall, G. J. H., 1967. *Geol. Survey Kenya Report*, **78**.
- Molnar, P. & Oliver, J., 1969. *J. geophys. Res.*, **74**, 2648.
- Presnall, D. C., Simmons, C. L. & Porath, H., 1972. *J. geophys. Res.*, **77**, 5665.
- Searle, R. C., 1970. *Geophys. J. R. astr. Soc.*, **21**, 13.
- Tolland, H. G. & Strens, R. G. J., 1972. *Phys. Earth Planet. Int.*, **5**, 380.
- Wyllie, P. J., 1971. *J. geophys. Res.*, **76**, 1328.